BMC Genomics

RESEARCH

Open Access

Genome-wide identification, characterization and expression analysis of key gene families in RNA silencing in centipedegrass

Siyu Liu[1†], Xiong Lei[2†], Wenlong Gou[3], Chunsen Xiong[1], Wei Min[4], Dandan Kong[1], Xiaoyun Wang[1], Tianqi Liu[1], Yao Ling[1], Xiao Ma[1] and Junming Zhao[1*]

Abstract

Background Argonaute (AGO), Dicer-like (DCL), and RNA-dependent RNA polymerase (RDR) are essential components of RNA silencing pathways in plants. These components are crucial for the generation and regulatory functions of small RNAs, especially in plant development and response to environmental stresses. Despite their well-characterized functions in other plant species, there is limited information about these genes and their stress responses in centipedegrass (*Eremochloa ophiuroides*), a key turfgrass species.

Results Using genome-wide analysis we identified 20 *AGO*, 6 *DCL*, and 10 *RDR* members in centipedegrass and provided a comprehensive overview of their characteristics. We performed the chromosomal location, gene duplication, syntenic analysis, conserve motif, gene structure, and *cis*-acting elements analysis. And conducted phylogenetic analyses to clarify the evolutionary relationships among the *EoAGO*, *EoDCL*, and *EoRDR* gene families. Three-dimensional modeling prediction of EoAGO, EoDCL, and EoRDR proteins supported the phylogenetic classification. Furthermore, we examined the expression patterns of these genes in different tissues (spike, stem, leaf, root, and flower) and under different stress conditions (cold, salt, drought, aluminum, and herbicide) using RT-qPCR. The results revealed that most of *EoAGO*, *EoDCL*, and *EoRDR* genes were upregulated in response to multiple abiotic stresses, while some exhibited unique responses, suggesting potential specialized regulatory functions.

Conclusion In this study, we performed a comprehensive genome-wide identification, and phylogenetic and expression pattern analyses of the *EoAGO*, *EoDCL* and *EoRDR* gene families. Our analysis provides a foundation for future research on the RNA silence elements of turfgrass, and affords scientific basis and insights for clarifying the expression patterns of *EoAGO*, *EoDCL* and *EoRDR* genes under adversity stress. Further functional validation and molecular breeding of these genes can be carried out for enhancing the stress resistance of centipedegrass.

Keywords *AGO*, *DCL*, *RDR*, Gene family, Centipedegrass, Abiotic stresses

[†]Siyu Liu and Xiong Lei contributed equally to this work .

*Correspondence:
Junming Zhao
junmingzhao163@163.com
Full list of author information is available at the end of the article

Introduction

Small noncoding RNAs in plants, such as microRNAs (miRNAs) and short interfering RNAs(siRNAs), comprise 21–24 nucleotides. These molecules regulate various aspects of plant growth and development, abiotic and biotic stress response, and signal transduction [1–3]. RNA interference (RNAi) is a conserved gene silencing process mediated by small RNAs (sRNAs), which regulates translational inhibition, RNA degradation, and chromatin modifications in eukaryotes [4]. This mechanism is essential in gene silencing and post-transcriptional regulation, with numerous RNAi technologies developed to address biotic and abiotic stress in plants [5, 6]. Previous studies have reported that sRNAs generation and functions are directly associated with the proteins encoded by three key RNAi gene families: the Argonaute (AGO), Dicer-like (DCL), and RNA -dependent RNA polymerases (RDR) [7, 8]. As fundamental elements of the RNAi mechanism, RDRs utilize RNA as a template to synthesize double stranded RNAs (dsRNA), while the RNase III-type DCLs are responsible for cleaving dsRNA into various sRNAs, including siRNAs and miRNAs. Subsequently, these sRNAs can bind to AGO family proteins and integrate into the core of RNA-induced silencing complexes (RISCs) [9–11]. The RISCs, guided by sRNAs, can recognize target genes through complementary base pairing and regulate gene expression at the post-transcriptional level [post-transcriptional gene silencing, (PTGS)] and the transcriptional level [transcriptional gene silencing, (TGS)] [12, 13]. In PTGS, dsRNA is processed by the DCL enzyme into siRNAs, which subsequently associate with AGO protein to form the RISC. The RISC complex subsequently recognizes and binds to complementary sequences on the target mRNA, leading to its degradation [14]. TGS involves modifying chromatin structure to inhibit gene expression, mediated by sRNAs that guide chromatin-modifying enzymes to specific genomic loci. Chromatin modification affects the gene silencing effect mediated by sRNA molecules by modifying the structure and accessibility of chromatin, including histone modification and DNA methylation [15]. miRNAs originate from single-stranded transcripts (pri-miRNAs) generated by RNA polymerase II, while siRNA is primarily processed from fully complementary dsRNA. Based on the mechanism of dsRNA production and the functional distinctions of siRNA, siRNA can be divided into various types, heterochromatic siRNAs (hc-siRNAs), phased secondary siRNAs (phasiRNAs) [16], trans-acting small interfering RNAs (ta-siRNAs), natural antisense siRNAs (nat-siRNAs), long siRNAs (lsiRNAs) [17, 18], long miRNAs (lmiRNAs) [19], and DCL-independent siRNA (sidRNAs) [20]. While miRNAs, ta-siRNAs, and nat-siRNAs mediate PTGS, hc-siRNAs, lmiRNAs, and sidRNAs direct DNA methylation thus inducing TGS [21].

The fundamental elements of the RNA silencing pathway, namely AGO, DCL, and RDR, have been identified in various species. For instance, a total of 20 genes were identified in Arabidopsis [22], 32 genes in rice [23], 28 genes in maize [24], and 26 in sorghum [25]. These studies have demonstrated that *AGO*, *DCL*, and *RDR* genes are essential in plant development, including flower and fruit development, and nutrient organs growth, including roots, stems, and leaves [26]. Additionally, they are essential in plant stress responses and defense against pathogens. Previous studies reported that some *AGO*, *DCL*, and *RDR* genes exhibit upregulated or downregulated expression changes in rice [23, 27], cucumber [28], and maize [29] in response to abiotic stresses, including drought, and high salt and temperatures.

Centipedegrass (*Eremochloa ophiuroides*) is an essential perennial (C4) warm-season diploid turfgrass species (2n = 2x = 18) belonging to the *Eremochloa* genus of the Poaceae family [30]. This grass species originates from the Yangtze River region in China; however, it is now widely distributed across southeast Asia, the southern United States, and the northern and eastern regions of Australia [31, 32]. Centipedegrass is one of the most popular turfgrasses because of its beautiful leaf color, excellent adaptability to nutrient-deficient soils, and minimal maintenance requirements, making it a preferred choice for lawn and slope preservation and landscaping purposes [33, 34]. Comparing with other warm-season turfgrasses, centipedegrass exhibits superior drought tolerance, robust disease resistance, and thrives in acidic to slightly alkaline soil conditions [35, 36].

Recently, many plants have been compelled to endure extreme environments including drought, salinity, cold and metal stresses, which seriously endangering their growth and development [28]. RNA silencing family genes expression is dynamically regulated during plant development and stress response, indicating the influential role of RNA silencing regulation in environmental signals response [1–3]. Therefore, performing a comprehensive analysis of the RNA silencing family in centipedegrass is essential. With the availability of a high-quality draft genome, it is possible for us to study on RNA silencing mechanism of centipedegrass. Further study on the regulatory mechanisms of RNAi, it may reveal the essential stress response genes that enhance stress tolerance, disease resistance, and overall quality in grass. In this study, we comprehensively analyzed *EoAGO*, *EoDCL*, and *EoRDR* genes, including the gene structures, conserved domains, duplication events, *cis*-acting elements and phylogenetic analysis. Furthermore, we examined the expression profiles of

these identified genes across various tissues and under diverse abiotic stress conditions. This study provided the basic genomic information and clarified the expression patterns of *EoAGO*, *EoDCL* and *EoRDR* genes under adversity stress. Through further functional validation and molecular breeding of these genes can be carried out for improving the stress resistance of centipedegrass.

Materials and methods

Plant genome sequence acquisition and identification of EoAGO, EoDCL and EoRDR gene family members

The genome sequence of Arabidopsis was obtained from the TAIR database (https://www.arabidopsis.org/), while genome sequences of other plants (sorghum, maize, and rice) were downloaded from the Phytozome database (https://phytozome-next.jgi.doe.gov/). The genome assembly and protein sequences of centipedegrass were obtained from the Figshare database (https://figshare.com/s/8256acffdb73bb050045) [37]. The Hidden Markov Model (HMM) profiles of the AGO, DCL, and RDR structural domains were AGO (PAZ PF02170, PIWI PF02171), DCL (DEAD PF00270, Helicase-C PF00271, Dicer-dimer PF03368, PAZ PF02170, RNaseIII PF00636), and RDR (RdRP PF05183). *EoAGO*, *EoDCL*, and *EoRDR* proteins in centipedegrass were identified using the default settings of HMMER 3.0 software (version 3.0), SMART (https://smart.embl.de/), Pfam(http://pfam-legacy.xfam.org/), and the Conserved Domain Database in NCBI were used to confirm finally resulted *EoAGO*, *EoDCL*, and *EoRDR* members. The resulting genes were named based on their phylogenetic relationship with the members of similar gene families in sorghum, maize, rice, and Arabidopsis. The ExPASy-ProtParam tool was used to determine the physio-chemical properties of the *EoAGO*, *EoDCL*, and *EoRDR* genes [38]. WoLF PSORT was used for subcellular localization predictions [39].

Multiple sequence alignment, phylogenetic analysis and classification of the EoAGO, EoDCL and EoRDR gene families

The EMBL-EBI-Clustal Omega tool with default settings was used to perform multiple sequence alignment of the predicted EoAGO, EoDCL, and EoRDR proteins and was viewed using the Jalview software (version 2.11) (https://www.jalview.org/) [40]. The neighbor-joining method with 1,000 times bootstrap-replicates in MEGA11 software was used to build the phylogenetic tree [41]. *EoAGO*, *EoDCL*, and *EoRDR* genes were assigned to different subgroups based on the classification of orthologous genes from Arabidopsis, sorghum, maize, and rice.

Chromosomal location, gene duplication, and syntenic analysis

Chromosomal location information of *EoAGO*, *EoDCL*, and *EoRDR* genes was obtained from GFF and sequencing files. The MCScanX was used to conduct gene duplication analysis [42, 43] and displayed by Circos plot [44]. The dual synteny plotter software (https://github.com/CJ-Chen/TBtools-II) was used to visualize the syntenic relationships between the *EoAGO*, *EoDCL*, and *EoRDR* genes of centipedegrass and other four plants (Arabidopsis, sorghum, maize, and rice). All these analyses were visualized using TBtools [45].

Conserve motif, gene structure, *cis*-acting elements analysis and 3-Dimensional structure prediction

The NCBI-CDD was demployed to obtain conserved domains of the EoAGO, EoDCL and EoRDR proteins. The exon–intron organizations of the *EoAGO*, *EoDCL*, and *EoRDR* genes were determined using TBtools. The PlantCare online software (https://bioinformatics.psb.ugent.be/webtools/plantcare/html/), visualized in TBtools, was used to predict the *Cis*-acting elements in the 2,000 bp upstream region of each gene.

SWISS-MODEL (https://swissmodel.expasy.org/) was used for EoAGO, EoDCL and EoRDR protein 3D structure prediction. The template selection is based on coverage and similarity (identity ≥ 30%). GMQE represents the accuracy and coverage of a model, with a credibility range of 0–1. A higher value indicates better quality.

Plant materials and stress treatments

Seeds of the centipedegrass cultivar 'Wuling' (provided by the Sichuan Academy of Grassland Science, Chengdu, China) were sown in square pots filled with quartz sand and cultivated under greenhouse conditions: temperature 23 /19 °C (12 h day/12 h night). After 2 months, a part of the seedlings underwent stress treatments: cold (4 ℃), drought (20% PEG-6000), salt (200 mmol L^{-1} NaCl), Al (100 mmol L^{-1} $AlCl_3$), and herbicide (6 mmol·L^{-1} glufosinate) stresses. Control plants were irrigated with ½ Hoagland nutrient solution. During the treatments, samples were collected at 0, 0.5, 1.5, 3, 6, 12, 24, 48, and 72 h during the treatments. The remaining seedlings cultivated under normal conditions were used to collect flower, stem, spike, root and leaf at during the flowering period of grasses. All collected samples were immediately frozen in liquid nitrogen for RNA extraction. Three samples at each treatment time point and tissue were taken for RNA extraction and RT-qPCR.

RNA isolation, cDNA synthesis and RT-qPCR expression analysis

Total RNA from centipedegrass was isolated with TRIzol reagent (Invitrogen, USA). The ABScript III Gdna Remover and Genious 2X SYBR qPCR Mix (Abclonal, Wuhan) were used for the synthesis of cDNA and RT-qPCR follow the manufacturer's protocol, the CXF Connect™ Real-Time System (Bio-Rad) was used for reactions. Based on the previous studies published by group [46], the most stable gene under different stresses was selected as the reference genes for calculating the gene expression using the $2^{-\Delta\Delta Ct}$ method [47], where the *UBC* (ubiquitin-conjugating enzyme) gene was used for cold and Al stress, the *MD* (malate dehydrogenase) gene was used for salt, drought stresses, and different tissues, and the *RIP* (60S ribosomal protein L2) gene was used for herbicide stress. Based on the location on the phylogenetic tree and the amino acid identity with each other, only seven *EoAGOs*, three *EoDCLs*, and four *EoRDRs* genes were selected for the RT-qPCR expression analysis. Primer software (version 5) was used to design the 14 primer pairs (Supplementary Table S4). RNA-seq data of centipedegrass under cold treatment were obtained from previous studies [35].

Results

Genome-wide identification of AGOs, DCLs and RDRs in centipedegrass

The HMM profiles of conserved domains were used to identify the *EoAGO*, *EoDCL* and *EoRDR* gene families. Analysis revealed 20 *EoAGO*s genes, 6 *EoDCL*s genes, and 10 *EoRDR*s genes in the centipedegrass genome database. The characteristics of the identified RNA silencing genes are summarized in Table 1.

The genomic length of 20 *EoAGO*s varied from 2241 to 3546 bp corresponding to *EoAGO*4c (evm.model.ctg136.122) and *EoAGO*7 (evm.model.ctg312.44), with their pI values exhibiting basic characteristics (pI value 8.66 ~ 9.59). The six *EoDCL*s ORF ranged from 2475 to 5811 bp corresponding to *EoDCL4* (evm.model.ctg.110.32) and *EoDCL1* (evm.model.ctg278.43). All EoDCL proteins exhibited acidic properties (pI value 5.94 ~ 6.49). The ORF length of EoRDRs varies between 1302 and 3624 bp corresponding to *EoRDR3b* (evm.model.ctg722.9) and *EoRDR6b* (evm.model.ctg599.18), respectively. Most *EoRDR*s exhibit acidic properties, while *EoRDR4b* and *EoRDR6b* demonstrate higher pI values of 8.15 and 8.3. Regarding subcellular localization predictions, 13 *EoAGOs* (65%) and 10 *EoRDRs* (100%) were predicted to be localized in the nucleus, while seven *EoAGOs* (35%) and six *EoDCLs* (100%) were predicted to be localized in the chloroplast.

Chromosomal localization, phylogenetic and syntenic analysis

We demonstrated the chromosomal distribution of the *EoAGO*, *EoDCL*, and *EoRDR* genes utilizing the GFF data from the centipedegrass genome (Fig. 1A). The *EoAGO*, *EoDCL*, and *EoRDR* genes exhibited uneven distribution across 9 chromosomes. We identified 20 *EoAGO* genes on almost all chromosomes except chromosome 7, while six *EoDCL* genes were solely located on chromosomes 1 2, and 4. Another 10 *EoRDR* genes were distributed among chromosomes 1, 5, 7, 8, and 9. Chromosome 4 contained the highest number of genes (eight), while chromosome 7 contained the fewest (one). Chromosome 1 contains all three kinds of genes. There were two pairs of *AGO* tandem duplications genes (*EoAGO1a*-EoAG*1b* and *EoAGO5c-EoAGO5d*) from chromosomes 3 and 6. Besides, *DCL* and *RDR* each possess a pair of tandem duplication genes (*EoDCL2a-EoDCL2b* and *EoRDR1a-EoRDR1b*) from chromosomes 4 and 8.

Furthermore, we also performed a collinearity analysis to identify duplication events in the *EoAGO*, *EoDCL*, and *EoRDR* genes (Fig. 1B). Only two pairs of segmental duplication genes were identified, both comprising *EoAGO* genes (*EoAGO1d-EoAGO1e* and *EoAGO5b-EoAGO5d*). Other *EoDCL* and *EoRDR* lack any segmental duplication genes. These findings indicate that the proliferation *EoAGO*, *EoDCL*, and *EoRDR* families may have been influenced by tandem and segmental duplication events, with tandem duplication possibly being the primary driving force.

The protein sequences of AGO, DCL, and RDR from four different plant species, including sorghum, maize, rice, and Arabidopsis, were used to create the phylogenetic tree to investigate the evolutionary relationship of the *EoAGO*, *EoDCL*, and *EoRDR* gene families. The *AGO*, *DCL*, and *RDR* gene families were categorized into several clades, based on the homology and classification within species, using Neighbor-joining method (NJ) approach with high bootstrap support (Fig. 2). The 20 *EoAGO* genes were separated into four different clades (Fig. 2A): Clade I comprised *AGO1* and *AGO10*, clade II comprised *AGO2* and *AGO7*, clade III comprised *AGO4* and *AGO6*, clade IV comprised *AGO5*, and clade V comprised *AGO18*. The *AGO18* member was absent in Arabidopsis. However, it existed in sorghum, maize, rice, and centipedegrass, indicating the specificity and similar evolution of *AGO18* in these grasses. Based on the phylogenetic analysis, all *DCL* genes were divided into four clades (Fig. 2B): clade I contained *EoDCL1*, clade II comprised *EoDCL2a* and *EoDCL2b*, clade III contained *EoDCL3a* and *EoDCL3b*, and clade IV contained *EoDCL4*. Besides, the 10 *EoRDR* genes were separated into four clades: clade I contained *EoRDR1a* and *EoRDR1b*, clade

Table 1 Basic information of *AGO*, *DCL* and *RDR* genes in centipedegrass

	Gene Name	Locus ID	Chromosomal location	ORF length (bp)	Mw (Da)	pI	Instability index	GRAVY	Subcellular localization
AGO	*EoAGO1a*	evm.model.ctg497.10	chr7:3,531,971–3,539,712	3321	121,829	9.55	49.29	-0.528	Nucleus
	EoAGO1b	evm.model.ctg498.5	chr7:3,648,204–3,655,953	3321	121,841.1	9.55	49.29	-0.524	Nucleus
	EoAGO1c	evm.model.ctg780.217	chr9:55,644,807–55,660,515	3318	122,401	9.53	49.87	-0.521	Nucleus
	EoAGO1d	evm.model.ctg391.46	chr5:102,512,987–102,520,102	2745	101,090.7	9.13	53.74	-0.438	Nucleus
	EoAGO1e	evm.model.ctg624.33	chr8:81,742,442–81,750,079	3132	115,567.5	9.47	52.77	-0.509	Nucleus
	EoAGO2	evm.model.ctg782.50	chr9:60,264,310–60,269,206	3069	110,606.8	9.40	44.48	-0.432	Nucleus
	EoAGO4a	evm.model.ctg573.10	chr6:71,861,539–71,866,868	2754	102,410.1	8.99	47.48	-0.373	Chloroplast
	EoAGO4b	evm.model.ctg21.9	chr1:21,004,110–21,012,014	2694	100,670.6	9.11	49.21	-0.380	Nucleus
	EoAGO4c	evm.model.ctg136.122	chr2:63,976,662–63,988,327	2241	84,242.57	8.73	51.45	-0.412	Chloroplast
	EoAGO4d	evm.model.ctg21.7	chr1:20,971,506–20,976,544	2637	97,980.53	9.16	44.73	-0.264	Chloroplast
	EoAGO5a	evm.model.ctg374.195	chr3:17,707,456–17,747,083	3366	121,870.4	9.62	49.92	-0.426	Nucleus
	EoAGO5b	evm.model.ctg382.112	chr4:5,126,642–5,134,952	3384	124,299.7	9.36	51.19	-0.406	Nucleus
	EoAGO5c	evm.model.ctg254.4	chr3:15,520,044–15,531,252	3465	126,281.1	9.46	46.94	-0.381	Nucleus
	EoAGO5d	evm.model.ctg253.270	chr3:15,614,325–15,622,564	2655	98,881.25	9.04	45.89	-0.317	Chloroplast
	EoAGO6	evm.model.ctg415.78	chr5:76,081,544–76,089,848	2523	94,313.97	9.29	47.11	-0.318	Nucleus
	EoAGO7	evm.model.ctg312.44	chr4:82,793,205–82,797,989	3546	132,281.8	9.59	48.88	-0.336	Chloroplast
	EoAGO10	evm.model.ctg402.94	chr5:93,406,197–93,421,012	2418	91,252.04	9.00	41.72	-0.334	Chloroplast
	EoAGO18a	evm.model.ctg194.36	chr3:91,247,450–91,252,794	3174	115,172.3	9.35	40.54	-0.497	Nucleus
	EoAGO18b	evm.model.ctg373.62	chr4:20,391,739–20,397,027	2784	103,422.4	9.04	39.57	-0.402	Nucleus
	EoAGO18c	evm.model.ctg462.4	chr5:24,108,058–24,113,635	2442	90,521.62	8.66	42.57	-0.351	Nucleus
DCL	*EoDCL1*	evm.model.ctg278.43	chr4:112,660,845–112,671,572	5811	216,143.1	6.09	43.02	-0.380	Nucleus
	EoDCL2a	evm.model.ctg366.102	chr4:26,660,222–26,676,924	3579	134,465.1	6.22	45.93	-0.116	Nucleus
	EoDCL2b	evm.model.ctg367.10	chr4:26,521,666–26,538,358	3705	139,249.9	6.49	45.42	-0.113	Nucleus
	EoDCL3a	evm.model.ctg62.68	chr1:80,081,933–80,090,656	4413	165,747	6.29	42.68	-0.260	Nucleus
	EoDCL3b	evm.model.ctg359.151	chr4:33,024,764–33,036,537	4986	186,822.8	6.18	44.80	-0.154	Nucleus
	EoDCL4	evm.model.ctg110.32	chr2:41,402,507-41,414,032	2475	93,886.41	5.94	43.44	-0.117	Nucleus

Table 1 (continued)

	Gene Name	Locus ID	Chromosomal location	ORF length (bp)	Mw (Da)	pI	Instability index	GRAVY	Subcellular localization
RDR	*EoRDR1a*	evm.model.ctg634.45	chr8:72,843,667–72,849,516	3339	127,570.1	6.84	39.82	-0.285	Chloroplast
	EoRDR1b	evm.model.ctg635.6	chr8:72,681,119–72,686,934	3339	127,563.1	6.86	39.69	-0.281	Chloroplast
	EoRDR2	evm.model.ctg769.18	chr9:45,305,488–45,311,415	3390	125,811.8	6.52	44.76	-0.200	Chloroplast
	EoRDR3a	evm.model.ctg722.8	chr9:7,674,410–7,683,240	1872	69,692.43	5.68	47.27	-0.355	Chloroplast
	EoRDR3b	evm.model.ctg722.9	chr9:7,683,242–7,698,311	1302	50,129.07	5.19	38.95	-0.407	Chloroplast
	EoRDR4a	evm.model.ctg7.29	chr1:4,513,777–4,572,529	2925	108,886.9	5.67	41.15	-0.269	Chloroplast
	EoRDR4b	evm.model.ctg7.31	chr1:4,576,824–4,588,094	3474	130,552.2	8.15	46.64	-0.399	Chloroplast
	EoRDR6a	evm.model.ctg398.176	chr5:97,820,643–97,823,154	1392	52,150.5	5.53	35.00	-0.326	Chloroplast
	EoRDR6b	evm.model.ctg599.18	chr7:21,144,141–21,148,060	3624	135,837	8.3	44.59	-0.241	Chloroplast
	EoRDR6c	evm.model.ctg38.11	chr1:42,871,533–42,876,902	3615	135,381.9	6.85	39.15	-0.260	Chloroplast

II contained *EoRDR2*, clade III contained *EoRDR3a*, *EoRDR3b*, *EoRDR4a,* and *EoRDR4b*, and clade IV contained *EoRDR6a*, *EoRDR6b,* and *EoRDR6c* (Fig. 2C). The *EoAGO*, *EoDCL* and *EoRDR* genes were named based on the location on the phylogenetic tree and combined with the blast result of amino acid identity with each other.

Synteny, which occurs within and between species, is another avenue for the rapid evolution of gene families. A comparative syntenic analysis was conducted using four representative species to further explore the evolutionary clues of the *EoAGO*, *EoDCL*, and *EoRDR* genes, three monocotyledonous plants (rice, maize, and sorghum), and one dicotyledonous plant (Arabidopsis) (Fig. 3). The findings revealed 29 syntenic pairs between centipedegrass and maize, followed by sorghum (28) and rice (23), while one syntenic pair was identified between centipedegrass and Arabidopsis. More syntenic pairs between centipedegrass and monocotyledons than dicotyledons suggests close evolutionary relationships between centipedegrass and other monocotyledons.

Conserved domains, multiple sequence alignment, gene structure, cis-elements analysis in the promoter regions and 3-Dimensional structure prediction

The conserved domains of the EoAGO, EoDCL and EoRDR proteins were identified demonstrating the structural domain conservatism and diversity among the proteins (Fig. 4A, Table S1). All EoAGO proteins possess four domains: ArgoN, PAZ, ArgoL2, and PIWI. Additional conserved domains, including ArgoL1, Gly-rich_Ago1 and ArgoMid, were identified in most EoAGOs. The additional Gly-rich domain in AGO1 of Arabidopsis, sorghum, and maize, was observed in EoAGO1 (EoAGO1a, EoAGO1b, EoAGO1c, and EoAGO1d). Furthermore, the multiple sequence alignment, indicates that the PIWI domain exhibits a structure similar to RNaseH, and is essential in cleaving target mRNA. This function is facilitated by a conserved metal-chelating motif known as Asp–Asp–His/Asp (DDH/D) (Fig. S1) [48, 49]. The sequence alignment results of the PIWI domains revealed that there were 11 EoAGO proteins exhibited the conserved DDH/H tetrad identical to those in AtAGO1 (Fig. S1). The DDD/H motif identified in EoAGO2 protein, is identical to AtAGO2 and AtAGO3 proteins. However, DDH/H motif is not essential and may be replaced into DDH/P and DDW/P, as observed in Arabidopsis, rice, maize and sorghum. The DDH/P motif was identified in EoAGO4a, EoAGO4b and EoAGO4d proteins, similar to the AtAGO6 and AtAGO8 proteins. The DDW/P motif was exclusively observed in EoAGO6 protein. Furthermore, the other four (EoAGO4c, EoAGO18a, EoAGO18b, and EoAGO18c) exhibited different deficiencies in PIWI domain catalytic residue(s) illustrated in Table S2.

The EoDCL proteins exhibited all the common domains found in the Dicer family, including DEAD, Helicase_C, Dicer_dimer, PAZ, two tandem RIBOc (RNaseIIIa and RNaseIIIb), and dsRM. However, EoDCL3a and EoDCL3b lacked the DSRM domain, and EoDCL4 lacked the PAZ, RIBIc, and DSRM domains (Fig. 4A). Besides,

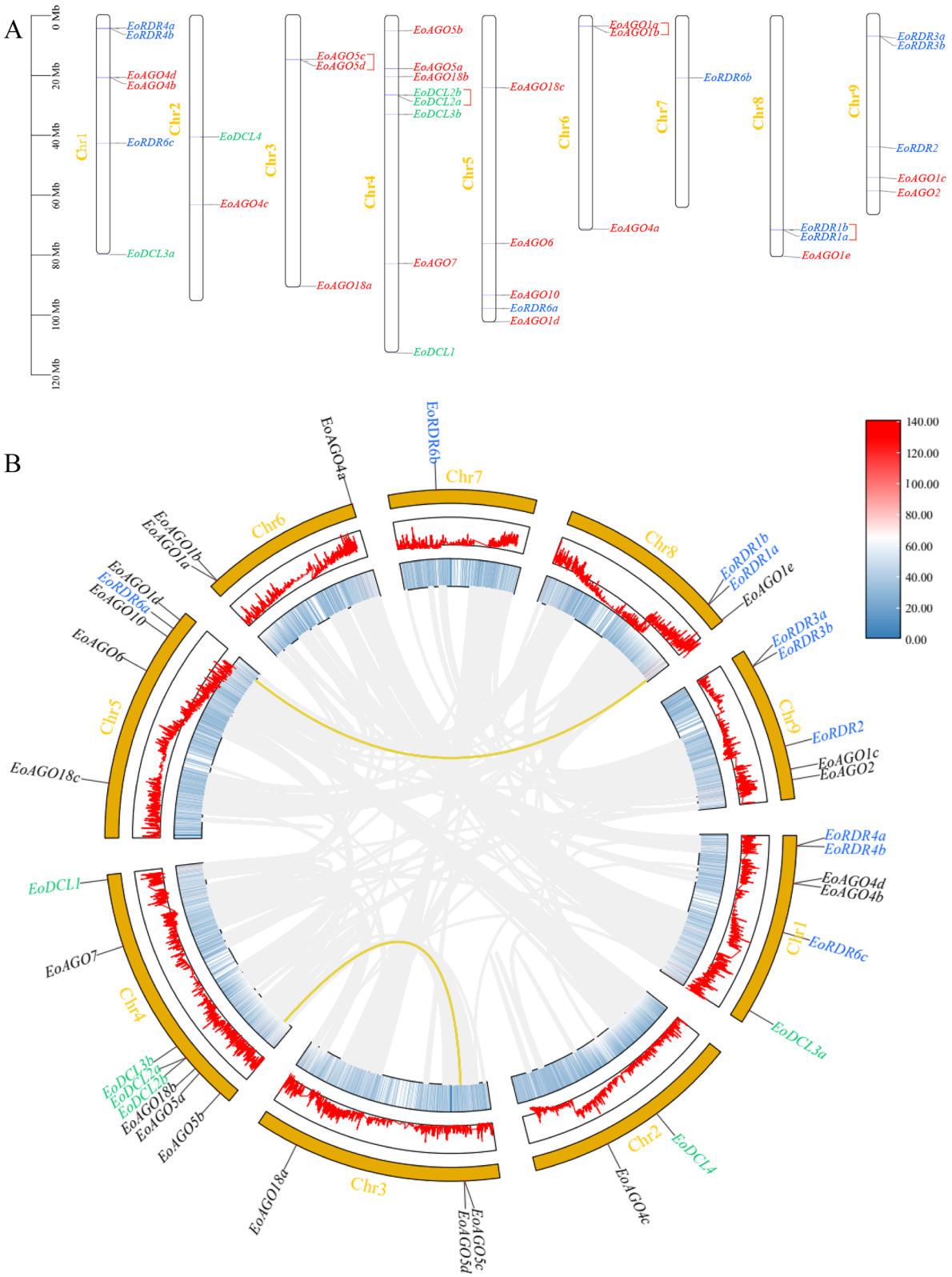

Fig. 1 **A** Distribution and location of *EoAGO*, *EoDCL*, and *EoRDR* genes on nine chromosomes. *AGO*: red, *DCL*: blue, *RDR*: green. The red-colored brackets indicate the tandem duplication gene pairs. **B** Schematic representations of the interchromosomal relationships of *EoAGO*, *EoDCL*, and *EoRDR* genes. The gray lines represent all synteny blocks in the centipedegrass genome. The yellow lines indicate the segmental duplication of gene pairs. The different colored box on the right represents the gene density of the heatmap in innermost circle

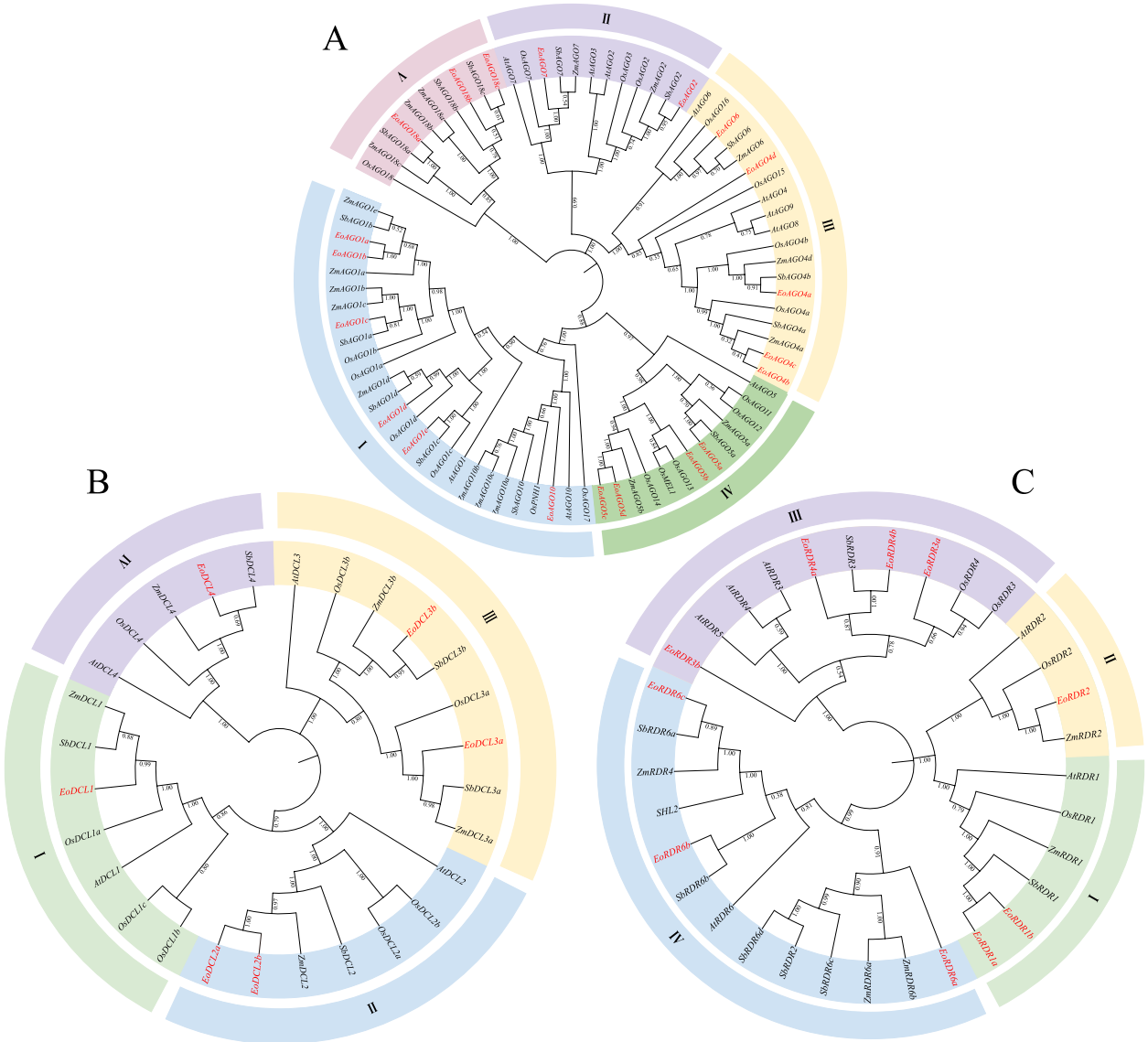

Fig. 2 Phylogenetic tree for *AGO*, *DCL* and *RDR* gene families from centipedegrass, Arabidopsis, rice, maize and sorghum. Gene families were separated into several clades, highlighted with colors. *EoAGO*, *EoDCL* and *EoRDR* genes were colored in red, **A**: *AGO*, **B**: *DCL*, and **C**: *RDR*

the EoDCL1 contained two DSRM domains, which were observed in DCL1 in Arabidopsis, maize, and sorghum. The sequence alignment demonstrated that all the EoDCL proteins, except EoDCL4, possess the RNase III catalytic sites within the two tandem RIBOc domains at the glutamate (E), aspartate (D), aspartate (D), glutamate (E) (EDDE) position (Fig. S1), a characteristic of plant DCL proteins [50, 51].

A conserved RdRP domain has been identified in all EoRDR proteins similar to the corresponding proteins in other plants (Fig. 4A). The sequence alignment of the EoRDR proteins identified the conserved DxDGD catalytic motif within the RdRP conserved domain, except for EoRDR3a, which lacks a portion of the DxDGD catalytic motif (Fig. S1) [52, 53].

Analyzing different exon–intron structures of the *EoAGO*, *EoDCL*, and *EoRDR* genes help us facilitates comprehension of their genetic variations and potential evolutionary processes (Fig. 4B). The coding sequences of the complete *EoAGO*, *EoDCL*, and *EoRDR* families were interrupted by introns. Most of the *EoAGO* genes exhibited an intron number ranging from 17 to 24, consistent across various in different groups. However, the *EoAGO2* and *EoAGO7* genes belong to clade II, possessing two

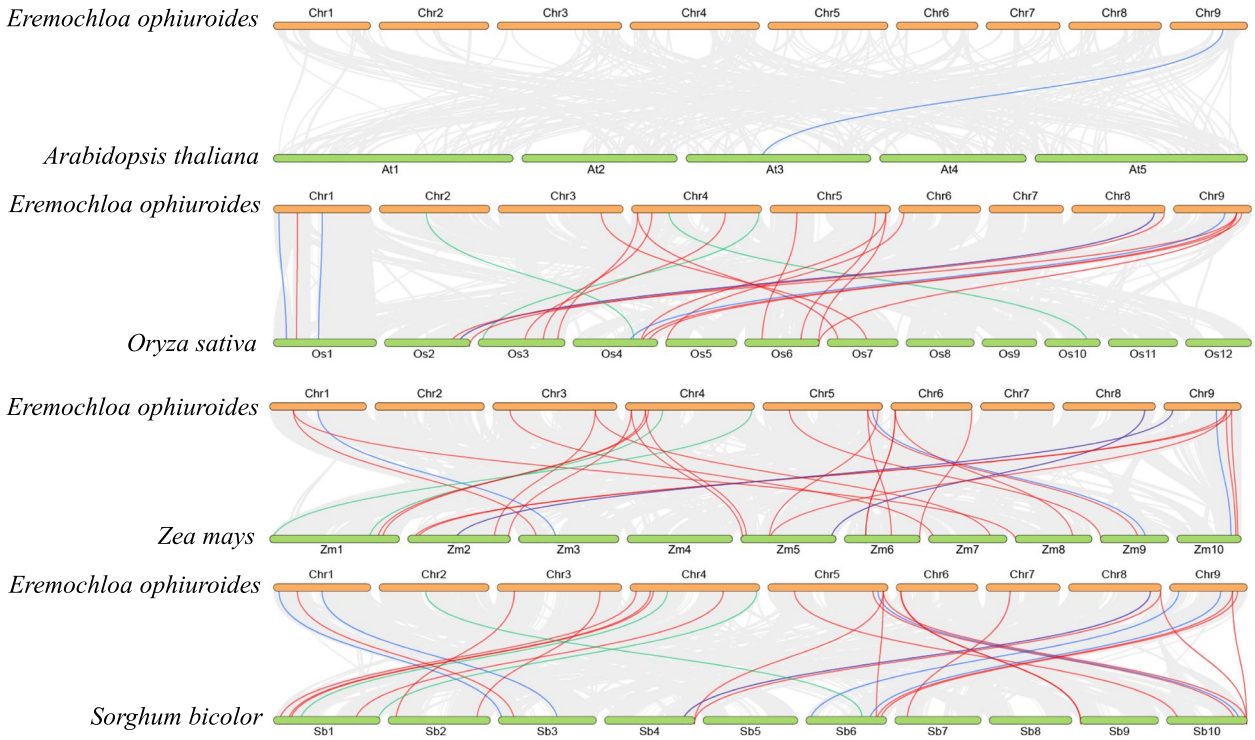

Fig. 3 Synteny analysis of *AGO*, *DCL* and *RDR* genes between centipedegrass and four representative plant species. Gray lines indicate the collinear blocks, whereas the colored lines indicate the syntenic *AGO* (red); *DCL* (green) and *RDR* (blue) gene pairs

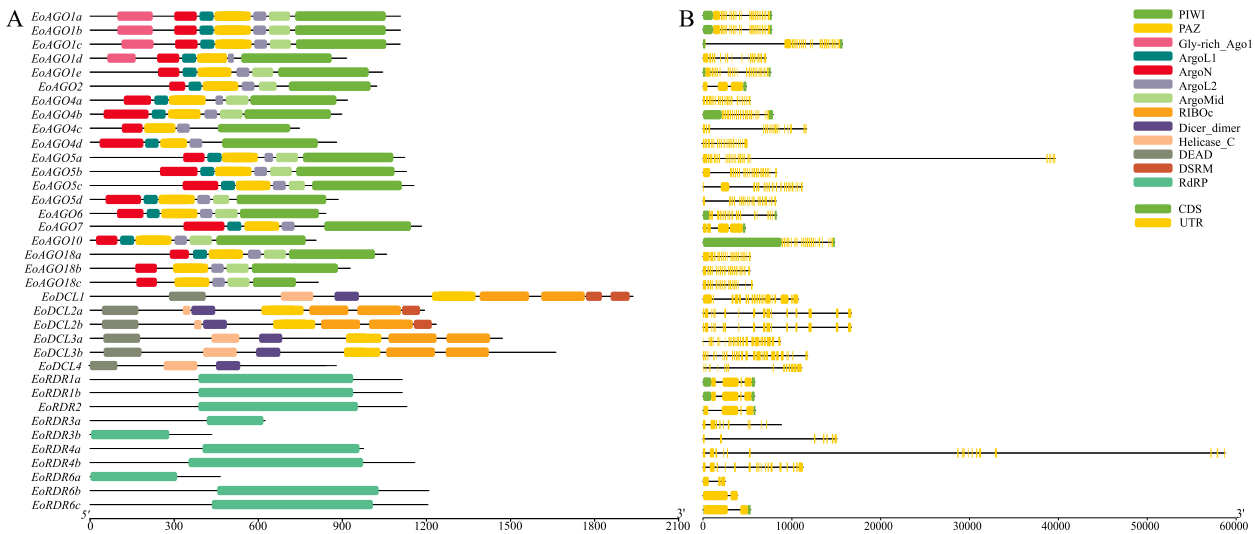

Fig. 4 Analysis of conserved domains and gene structure of *EoAGO*, *EoDCL* and *EoRDR* genes. **A** Conserved domain composition analysis. **B** Gene structure analysis

and three introns, respectively. Regarding *EoDCL*s, the introns number ranges from 14 to 25. Most *EoRDR*s contained 1–3 introns, while clade III (*EoRDR3* and *EoRDR4*) contained 6–17 introns. The intron number of *EoAGO*, *EoDCL*, and *EoRDR* genes exhibited significant variation between clades but remained relatively conserved among members in the same clade, similar to that of other plants.

We analyzed 34 *cis*-element elements across all members of the *EoAGO*, *EoDCL*, and *EoRDR* genes families,

categorizing them into three groups: abiotic and biotic stress, phytohormone responsiveness, plant growth and development (Fig. 5). Among the genes, *EoAGO*5b exhibited the highest number of *cis*-acting elements, while *EoRDR3a* exhibited the fewest. Light-responsive, abs*cis*ic acid-responsiveness elements, and MeJA-responsiveness elements were the most prevalent in the *EoAGO*, *EoDCL*, and *EoRDR* families (Fig S2, Table S3). Other *cis*-acting elements associated with meristem expression, auxin responsiveness, defense and stress responsiveness, low-temperature responsiveness, and wound responsiveness were identified. The findings indicate that *EoAGO*s, *EoDCL*s, and *EoRDR*s are essential in regulating processes, including photoperiodic control of flowering, hormone signaling pathways (MeJA, salicylic acid, and abscisic acid), and stress responses.

The three-dimensional structures of the EoAGO, EoDCL, and EoRDR proteins were predicted using the SWISS-MODEL [54] (refer to Fig S3 and Table S5). Each target exhibited greater than 30% identity with the template, a threshold indicative of successful modeling, as noted in the advancements of homology protein structure modeling. The GMQE values, ranging from 0.54 to 0.92, signified the high-quality nature of all the models. The majority of the models employed for predicting the 3D structures of EoAGO, EoDCL, and EoRDR were derived from rice, maize, and sorghum species, highlighting the close genetic affinity between centipedegrass and these species. This proximity suggests the possibility of functional parallels among the genes.

Expression analysis of EoAGO, EoDCL, and EoRDR genes in different tissues

We selected seven *EoAGO*, three *EoDCL*, and four *EoRDR* genes from different phylogenetic tree clades to analyze their expression using RT-qPCR in other tissues, including stem, spike, root, leaf, and flower. All selected genes were expressed, however, *EoAGO2*, *EoDCL3b*, and *EoRDR1a* were expressed in all tissues (Fig. 5). Furthermore, all selected genes were expressed in stem, spike,

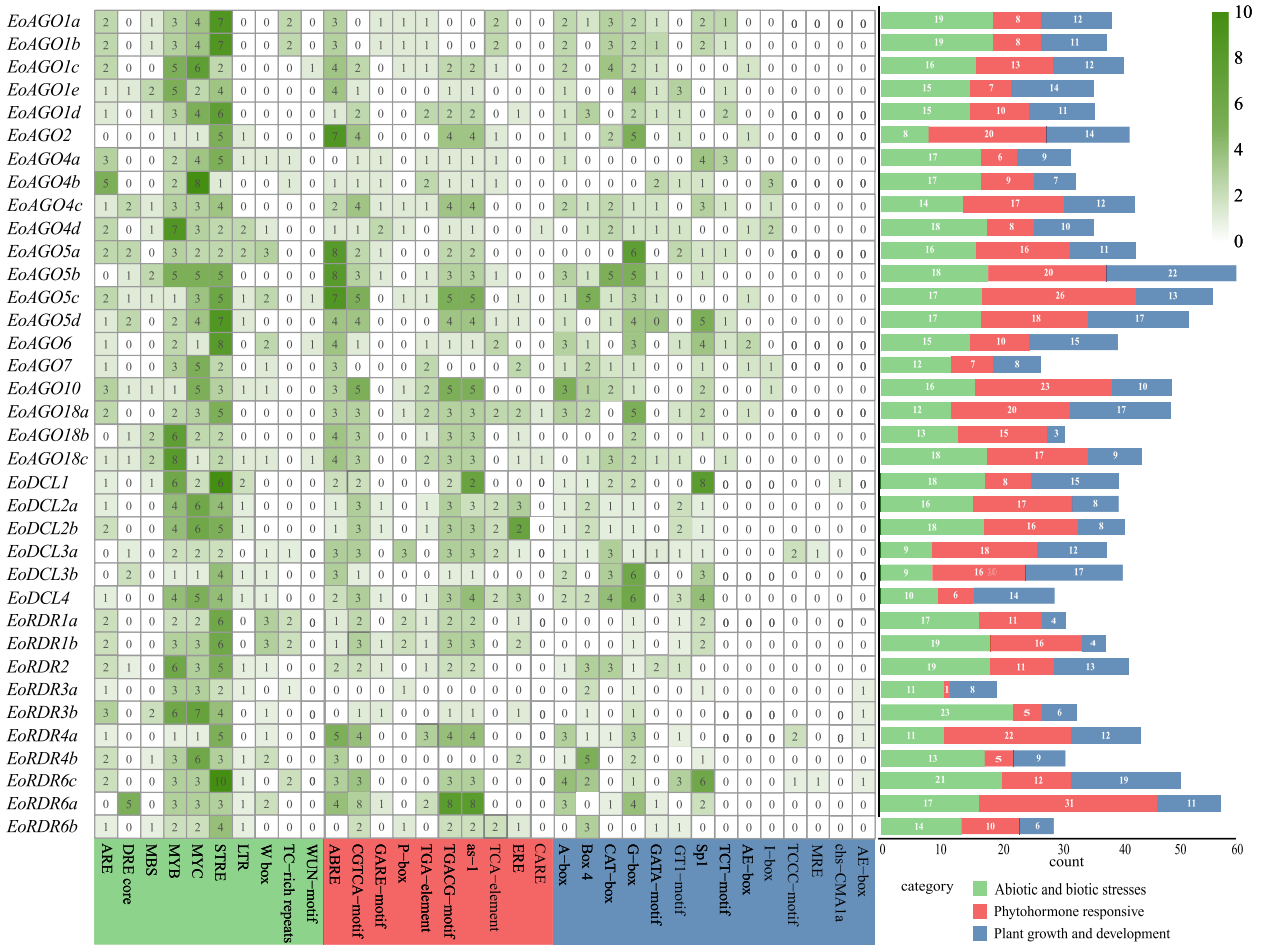

Fig. 5 The *cis*-acting elements distribution of types and numbers analysis of *EoAGO*, *EoDCL* and *EoRDR* gene promoters. The green gradient legend indicates the number of *cis*-acting elements

and leaf with *EoAGO1d*, *EoAGO5d*, and *EoDCL1* demonstrating the highest expression level, respectively. In addition, numerous genes exhibited low expression in root and flower, while *EoAGO1d* and *EoDCL2a* demonstrated the highest expression levels, respectively. Among the *EoAGO* genes, five genes (*EoAGO1d*/*4*/*5d*/*6*/*10*) exhibited no expression in the flower, while *EoAGO2/7* exhibited higher expression levels in other tissues. Most *EoAGO* genes exhibited lower spike and root expression levels than in stem and leaf. However, *EoAGO5d* exhibited higher expression in spike and root than in stem and leaf. Of the three *EoDCL* genes (*EoDCL1*/*2a*/*3b*), exhibited significantly higher flower expression levels. However, they did not express themselves in the root. Among *EoRDR* genes, *EoRDR1a* was expressed in all five tissues, and *EoRDR1a* and *EoRDR6b* exhibited high expression levels in the flowers especially for *EoRDR6b*. Another two genes (*EoRDR2/3b*) exhibited higher expression in the stem than in the spike and leaf, however, they exhibited no detectable expression in root and flower tissue.

Expression analysis of EoAGO, EoDCL, and EoRDR genes under five abiotic stresses

We analyzed the expression pattern of seven *EoAGO*, three *EoDCL*, and four *EoRDR* genes under various treatments, including cold, salt, PEG, Al, and herbicide stresses. The results revealed that all *EoAGO*, *EoDCL*, and *EoRDR* genes are differentially expressed under five abiotic stresses (Fig. 7).

Under cold stress, five *EoAGO*, one *EoDCL*, and three *EoRDR* genes exhibited significant upregulation at 3 h (*EoAGO6*, *EoRDR3b*) or 6 h (*EoAGO1d*/*4*/*5d*/*6*/*10*, *EoDCL3b*, *EoRDR2/6b*). Subsequently, the expression levels declined ($p < 0.05$) (Fig. 7A). Moreover, we employed existing RNA-seq datasets to examine the transcript levels of *EoAGO*, *EoDCL*, and *EoRDR* genes in response to cold treatments. We identified ten *EoAGO*, five *EoDCL*, and six *EoRDR* genes using the protein blast of NCBI (identify > 90%). The findings indicated that a subset of *EoAGO*, *EoDCL*, and *EoRDR* genes exhibited differential expression patterns in response to cold treatments (Fig. 7F), which was partially consistent with the RT-qPCR findings, including *EoAGO1a/4a/6/10*, *EoDCL*1/*3b*, and *EoRDR2/3b/6b* genes.

All selected genes exhibited varying degrees of upregulation at 6, 12, and 24 h under salt treatment, followed by a subsequent decrease in expression levels ($p < 0.05$), and *EoAGO4a*, *EoAGO6*, *EoDCL1*, *EoRDR2*, and *EoRDR3b* exhibited a significant upregulation (Fig. 7B). Regarding PEG treatments, the *EoAGO4A/5d/10*, *EoDCL2a*, and *EoRDR6b* significantly expressed at 3 h ($p < 0.05$), and followed by rapid decline (Fig. 7C). Additionally, other genes expression decreased with prolonged exposure time, especially for *EoAGO2* and *EoRDR3b* after PEG treatment for 3 h. For Al treatment, *EoAGO1d/2/4a/5d/7/10*, *EoDCL1/2a/3b*, and *EoRDR1/2/3* were downregulated after treatment for 1.5 h ($p < 0.05$). However, most of them were upregulated again after treatment for 12 h (Fig. 7D). Regarding herbicide stress, almost all selected genes were induced at 12 h ($p < 0.05$), and *EoAGO10* and *EoDCL2a* were significantly expressed. Moreover, most of these genes were decreased at 24 h ($p < 0.05$) by herbicide treatment (Fig. 7E).

Discussion

RNA silencing is a regulatory mechanism for gene expression regulation and a defense strategy common among eukaryotes. Moreover, it is essential in plant stress physiology. Plants can process diverse sRNAs through different *RDR-DCL-AGO* gene interactions, thereby indirectly regulating multiple biological pathways [16, 55]. This study conducts a comprehensive genome-wide analysis of *EoAGO*, *EoDCL*, and *EoRDR* genes in centipedegrass. The study investigated the correlation between these genes and their equivalents in other grass species, and their expression patterns in response to various abiotic stress factors.

Duplication events, evolution relationships and expression characteristics among AGO family in centipedegrass

AGO is an essential component of RISC and regulates plant leaf polarity differentiation. With the complete sequencing of plant genomes, the *AGO* gene family has been identified in many plants, including rice (19 members) [23], maize (18 members) [24], sorghum (14 members) [25], Arabidopsis (10 members) [22], and so on. In this study, 20 *AGO* genes were found from the centipedegrass genome, indicating the diversification and duplication events of *AGO* genes have occurred during evolution [56]. Previous studies reported that clade I, II and V all belong to AGO1/5/10/18 group [57, 58]. Arabidopsis contains *AGO1* and one *AGO10*, while centipedegrass has five AGO1 homologs, similar to the four homologs in rice and sorghum, and five in maize, which suggest redundant and specialized functions [59]. In the *AGO1* gene in centipedegrass, we identified one pair of tandem duplication genes (*EoAGO1a-EoAGO1b*) and one pair of segmental duplication genes (*EoAGO1d-EoAGO1e*), indicating the significant role of duplication events in *AGO1* gene expansion. The *AGO5* family was expanded in Poaceae plants [60], with five homologs in rice, and three each in maize and sorghum, indicating a conserved role in the 21-nt phasiRNA pathway, which is essential for developmental processes and male reproductive ability [61]. Tandem duplication genes (*EoAGO5c-EoAGO5d*) and segmental duplication

genes (*EoAGO5b-EoAGO5d*) were identified among the *EoAGO5* genes. The AGO18 family, which is grass-specific, is essential in plant reproduction and viral defense. For instance, the *AGO18* gene in rice could induced by viral infection, while *EoAGO18a/18b/18c* was not detected in centipedegrass [27, 62]. In the AGO2/7 group in clade III, it was observed that *AGO2* probably diverged from *AGO7* from their common ancestor of seed plants, as evidenced by the different catalytic triad sequences (DDH in AGO7 and DDD in AGO2) (Fig. S1, Table S2). This change from H to D in the catalytic triad may indicate functional divergence. *AGO7* is highly conserved and known to bind miR390, which initiates the generation of TAS3-derived trans-acting siRNAs (tasiRNAs) that regulate auxin response factors (ARF) in flowering plants [63, 64]. Clade IV belongs to the AGO4/6/8/9 group. *EoAGO4a/4b/4c/4d* and *EoAGO6* were contained in this clade, without *AGO7* and *AGO9* in centipedegrasss, similar in rice and sorghum. *EoAGO4* gene exhibits more complex evolutionary patterns, while *EoAGO6* is highly conserved, presumably due to involvement in different sRNA pathways. The AGO4/6/8/9 group should be classified into AGO4 and AGO6 clades, representing two distinguishable clades in plants, consistent with findings in centipedegrass and other Poaceae species [62]. Among the seven *EoAGO* genes for RT-qPCR, only *EoAGO2* and *EoAGO7*, clade III member, were expressed in flower, suggesting their involvement in the flower development pathway in centipedegrass. In addition, most *EoAGO* genes exhibited higher expression levels in the stem and leaf, while demonstrating lower expression in the root (Fig. 6). *EoAGO5d* exhibited high expression in the spike, indicating active involvement in reproductive tissues. In Arabidopsis, *AGO5* was reported to show high expression during all stages of flower and seed formation [63]. In response to cold stress, five out of seven *EoAGO* genes (*EoAGO1d*/*4a*/*5d*/6/*10*) were upregulated at 6 h and subsequently declined (Fig. 1a), mirroring the expression pattern of *ZmAGO1a/1b/4/5a/5/10b* in maize [29]. The overall expression patterns were largely in line with the RNA-seq data analysis (Fig. 7F). Under salt treatment, all *EoAGO* genes responded at 6 h or 24 h, exhibiting varying gene expression patterns. As for PEG treatment, *EoAGO4a/5d/10* were significant upregulated, suggesting their essential roles in gene regulation during drought stress. Moreover, all seven *EoAGO* genes displayed varying response levels under Al and herbicide treatments, although further research is needed to confirm these results.

DCL family in centipedegrass demonstrated distinct characteristics and specific expression in flower

DCL is an essential element in sRNA biogenesis, originally discovered in animals [65]. A previous study suggest that the plant DCL protein emerged after the plant-animal split but before the monocot-dicot divergence around 150 million years ago [66]. In Arabidopsis, four DCL proteins, named DCL1 to DCL4, have specialized

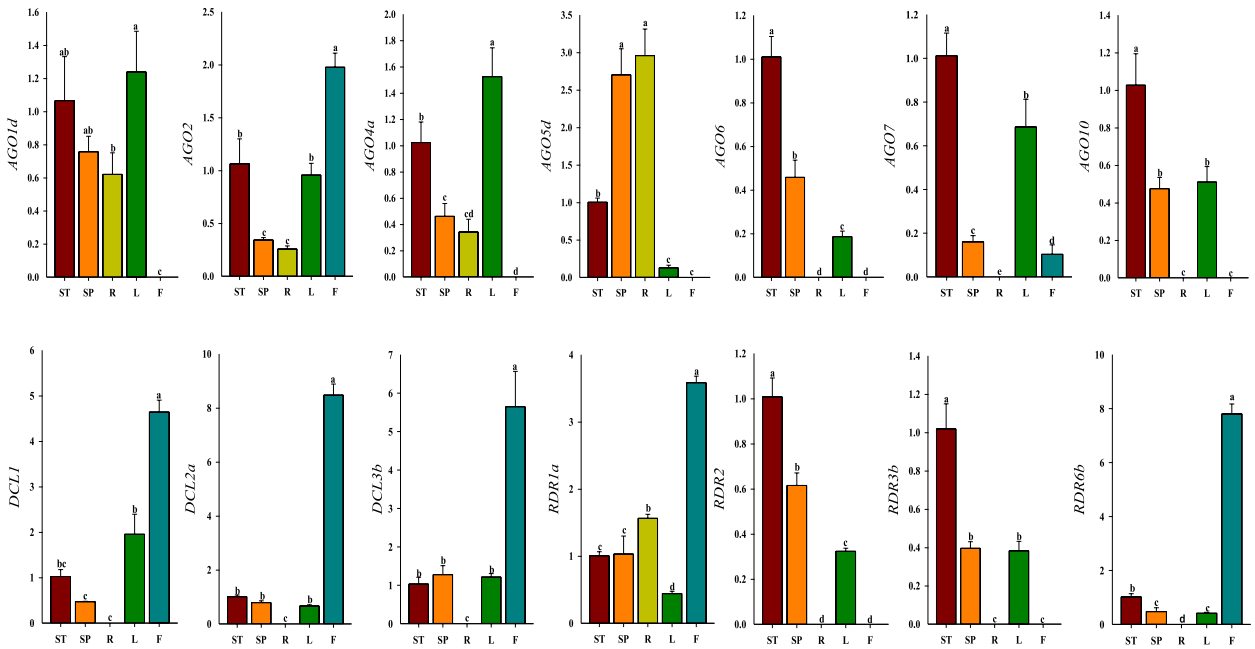

Fig. 6 The expression patterns of 14 *EoAGO*, *EoDCL* and *EoRDR* genes in the stem (ST), spike (SP), root (R), leaf (L), and flower(F) by RT-qPCR assay. Lowercase letter(s) indicate significant differences ($p < 0.05$, Duncan) among the tissues

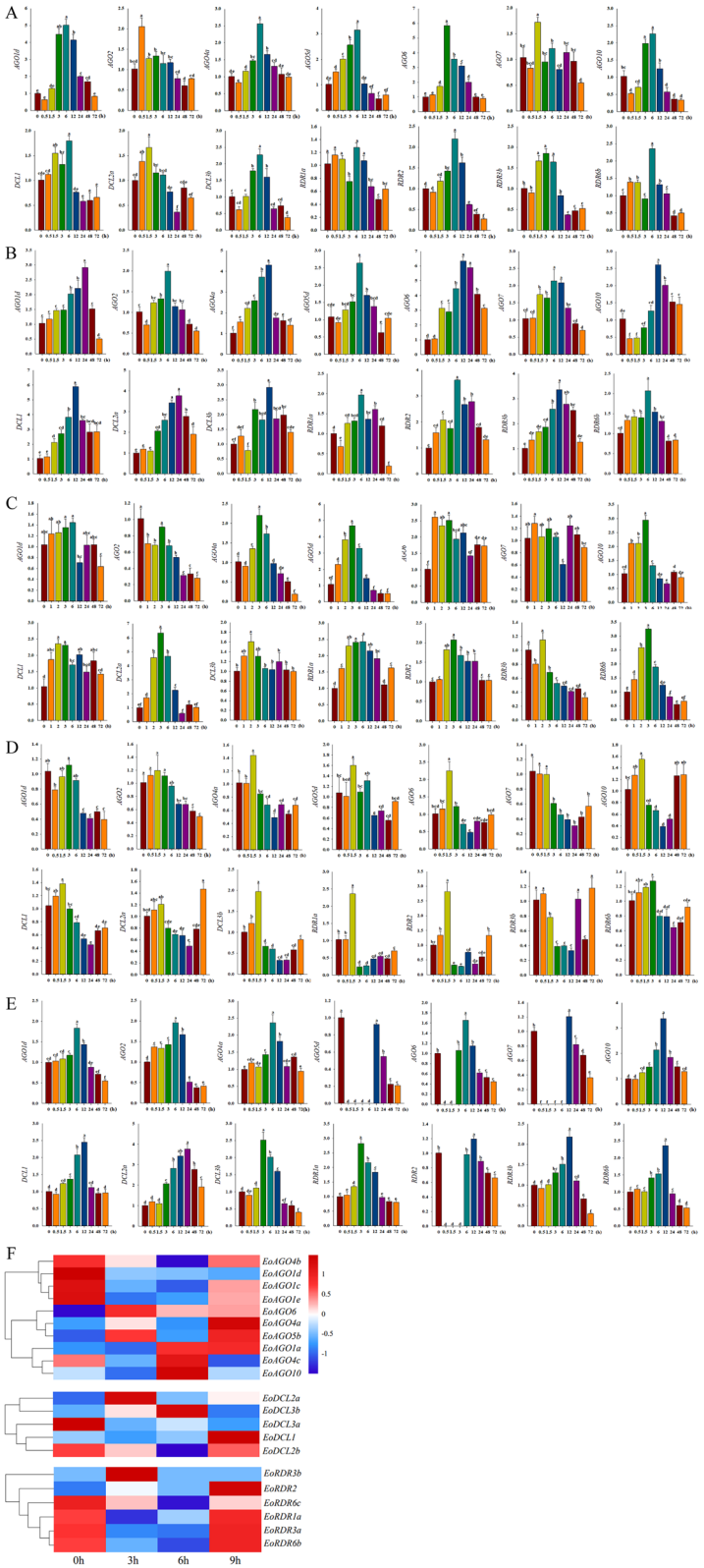

Fig. 7 Gene expression of *EoAGO*, *EoDCL* and *EoRDR* genes under **A** cold, **B** salt, **C** drought, **D** Al and **E** herbicide stress conditions analyzed using RT-qPCR assay after treatment for 0, 0.5, 1.5, 3, 6, 12, 24, 48, 72 h. Small letter(s) indicated significant differences ($p < 0.05$, Duncan) between different time stages. **F** *EoAGO*, *EoDCL* and *EoRDR* genes expression under cold stress based on RNA-seq data

functions in the sRNAs biogenesis [67]. For instance, DCL1 is mainly involved in the biogenesis of miRNAs [68], the function loss of *OsDCL1* affects miRNA accumulation and causes developmental defects in rice [69], DCL2 is associated with viral dsRNA processes, DCL3 is necessary for color modification and long-distance RNAi signaling [70, 71], and DCL4 regulates plant development by transacting on the biogenesis of siRNAs (ta-siRNAs) and reproductive phasiRNAs [72]. In the evolution of monocot plants, whole-genome duplications (WGD) greatly affect the growth of the *DCL* gene family [73]. Studies have demonstrated that grass ancestors had one WGD and two chromosome fusion events [74, 75]. In rice, the *DCL* gene experienced functional differentiation after the ρ-WGD event, helping with virus defense and gene regulation [74]. In addition, the *DCL* gene may evolve new functions through subfunctionalization and neofunctionalization [76]. It was reported in rice [77] and maize [78] that *DCL3b* (also called *DCL5*) emerged and evolved in monocots and is involved in producing reproductive phasiRNAs in anthers. In this study, we identified six *EoDCL* genes distributed across four clades, each containing at least one *EoDCL* member (Fig. 2B). Clade II contains two *DCL2* genes, similar to the *OsDCL2* genes. *EoDCL2a* and *EoDCL2a* were considered tandem duplication genes because of their proximity on chromosome 4 and 96% amino acid sequence identity (Fig. 1A), suggesting that gene duplication events contributed to *DCL2* gene expansion. Clade III own two *DCL3* members, *EoDCL3a* and *EoDCL3b*, which exhibit low similarity, consistent with the observations in sorghum, rice, and maize but contrasting with those in Arabidopsis and soybean [25]. This indicates that the emergence of the *DCL3b* paralog in monocots occurred after the split of monocots and dicots [79]. The function of *DCL3a* and *DCL3b* in rice and maize is diversified; *OsDCL3a* and *ZmDCL3*a are involved in hc-siRNAs biogenesis, however, *OsDCL3a* and *ZmDCL3b* (*ZmDCL5*) are engaged in 24-nt phasiRNAs biogenesis [77, 78]. Therefore, *EoDCL3b* may be designated as *EoDCL5* within a new clade. However, the functional divergence and expression patterns between *EoDCL3a* and *EoDCL3b* require further investigation. Although plants evolved four different DCL groups, their functions overlap and can compensate for each other without one [80]. Expression patterns indicate that three selected *EoDCL* genes exhibit consistent expression across all tissues, with high expression levels in flowers (Fig. 6). In Arabidopsis, DCL genes are essential in inducing flowering, as *dcl1/dcl3* mutants exhibited delayed flowering [81]. Consequently, *EoDCL* genes may be crucial in flowering and related miRNA and siRNA biogenesis. Regarding abiotic stresses, *EoDCL1/2a/3b* exhibited significant upregulation under cold, salt, and herbicide treatments, while all the expressions were downregulated under Al treatment (Fig. 7). The changes in *EoDCL1* and *EoDCL3b* expression levels under cold treatment were consistent with RNA-seq dataset results findings (Fig. 7F). *EoDCL2a* exhibited significant upregulation under drought treatment, similar to *ZmDCL2/3b* in maize [24]. These results revealed that the three *EoDCL1/2a/3b* genes could be regulated by various abiotic stresses.

RDR family in centipedegrass own a conserved domain and demonstrated potential function in reproductive growth

RDR is essential for siRNA biogenesis as it facilitates the conversion of single-stranded RNA into double-stranded RNA through the RdRP conserved domain. According to the phylogenetic tree analysis, RDRs can be classified into four groups in centipedegrass (Fig. 2 C). Clade I contains tandem duplication genes (*EoRDR1a-EoRDR1b*) in centipedegrass, while other species have one member (Fig. 2). It was found that *RDR1/2* were sister genes to *RDR6*, mainly involved in virus defense response [82]. Besides, *RDR2* has been associated with DNA methylation and repressive chromatin modifications in several plant species including Arabidopsis and maize [29, 83, 84]. We identified three *RDR6* orthologues in centipedegrass, similar to those in maize, indicating a conserved role of *RDR6* in plants with the production of highly conserved 21-nt tasiRNAs pathway [85]. Furthermore, *RDR6* participates reproductive phasiRNAs generation, with *EoRDR6b* exhibiting significantly high expression in flowers, indicating a potential role in reproductive growth in centipedegrass (Fig. 6). *RDR3* considered ancestral to other RDR types [27]. Four *EoRDRs* members (*EoRDR3a/3b/4a/4b*) were identified in clade III. However the specific function of *RDR3* remains unknown. Under various abiotic stresses, all four *EoRDRs* exhibited different responses (Fig. 7). The *EoRDR2*, *EoRDR3b* and *EoRDR6b* exhibited low expression levels in various tissues, but they were significantly upregulated under drought stress, indicating a potential function in response to specific environmental stresses.

Conclusion

We identified and characterized 20 EoAGO, 6 EoDCL and 10 EoRDR genes in the centipedegrass genome, comprehensively analyzing their critical roles in RNA silencing mechanisms. A total of two tandem and two segmental duplication pairs were identified in the AGO family, contributing to the gene expansion. EoDCL1/2a/3b and EoRDR6b exhibited high flowers expression levels, suggesting a significant role in flowering. Furthermore, some of the EoAGO, EoDCL and EoRDR genes could be regulated by

various stresses such as cold, drought, salt, Al, and herbicide, indicating that these genes play an essential role in the stress resistance of centipedegrass. Combining RNA-seq data analysis with RT-qPCR findings, reavealed that EoAGO4a/6/10, EoDCL2a/3b and RDR3b exhibited significant responses under cold stress. Future research will focus on the functional verification of these cold responsive genes, and through genetic transformation and breeding programs to cultivate new varieties of centipedegrass with higher stress resistance, laying the foundation for creating new germplasm.

Supplementary Information

The online version contains supplementary material available at https://doi.org/10.1186/s12864-024-11062-y.

Additional File 1: Fig S1. Sequences alinement of AGO, DCL and RDR genes. Fig S2. Promoter classification and proportion analysis of EoAGO, EoDCL and EoRDR genes. Fig S3. Three-dimensional (3D) protein structures of EoAGO, EoDCL and EoRDR proteins. Table S1. The alignment details and features of conserved domains of EoAGO, EoDCL and EoRDR genes. Table S2. AGO proteins with missing catalytic residue(s) in PIWI domains. Table S3. Promoter analysis of EoAGOs, EoDCLs and EoRDRs. Table S4. Primers used in the RT-qPCR analysis. Table S5. The detailed information of the predicted three-dimensional (3D) proteins.

Authors' contributions

SY L and JM Z experimental conception and design. SY L, X L, X M, and JM Z identification and bioinformatic analysis. XY W, TQ L, and W M material cultivation and treatments. SY L, CS X, DD K, and Y L genes expression by RT-qPCR. SY L, X L original manuscript preparation. JM Z and X L experiments supervision and manuscript revision. JM Z and X L funding acquisition. All authors have read and approved the final manuscript.

Funding

This research was funded by the National Natural Science Foundation of China (32071885), the Sichuan Science and Technology Program (2024YFHZ0300) and the Sichuan Forestry and Grassland Science and Technology Innovation Team Funding (CXTD2024005).

Data availability

The datasets presented in this study can be found in online repositories. The names of the repository/repositories and accession number(s) can be found below: https://figshare.com/s/8256acffdb73bb050045.

Declarations

Ethics approval and consent to participate

All the experimental research and field studies on plants (either cultivated or wild), including the collection of plant material, were carried out in accordance with relevant institutional, national, and international guidelines and legislation.

Consent for publication

Not applicable.

Competing interests

The authors declare no competing interests.

Author details

[1]College of Grassland Science and Technology, Sichuan Agricultural University, Chengdu, Sichuan 611130, China. [2]Sichuan Academy of Grassland Science, Chengdu, Sichuan 611731, China. [3]School of Life Science and Engineering, Southwest University of Science and Technology, Mianyang, Sichuan 621010, China. [4]Aba County Bureau of Science, Technology and Agriculture and Animal Husbandry, Aba, Sichuan 624600, China.

Received: 5 June 2024 Accepted: 18 November 2024
Published online: 26 November 2024

References

1. Chen X. Small RNAs and their roles in plant development. Ann Rev Cell Dev. 2009;25:21–44.
2. Lu S, Ying S, Vincent LC. Stress-responsive microRNAs in Populus. Plant J. 2008;55(1):131–51.
3. Yu S, Wang JW. The Crosstalk between MicroRNAs and Gibberellin Signaling in Plants. Plant Cell Physiol. 2020;61(11):1880–90.
4. Finnegan EJ, Matzke MA. The small RNA world. J Cell Sci. 2003;116(23):4689–93.
5. Gualtieri C, Leonetti P, Macovei A. Plant miRNA cross-kingdom transfer targeting parasitic and mutualistic organisms as a tool to advance modern agriculture. Front Plant Sci. 2020;11:930.
6. Bordoloi KS, Agarwala N. MicroRNAs in plant insect interaction and insect pest control. Plant Gene. 2021;26.
7. Carrington JC, Ambros V. Role of microRNAs in plant and animal development. Science. 2003;301(5631):336–8.
8. Voinnet O. Origin, Biogenesis, and activity of plant microRNAs. Cell. 2009;136(4):669–87.
9. Valencia MA, Liu J, Hannon GJ, Parker R. Control of translation and mRNA degradation by miRNAs and siRNAs. Genes Dev. 2006;20(5):515–24.
10. Pratt AJ, MacRae IJ. The RNA-induced silencing complex: A versatile gene-silencing machine. J Biol Chem. 2009;284(27):17897–901.
11. Fei Q, Xia R, Meyers BC. Phased, secondary, small interfering RNAs in posttranscriptional regulatory networks. Plant Cell. 2013;25(7):2400–15.
12. Peters L, Meister G. Argonaute proteins: mediators of RNA silencing. Mol Cell. 2007;26(5):611–23.
13. Vaucheret H. Plant argonautes. Trends Plant Sci. 2008;13(7):350–8.
14. Guo Z, Li Y, Ding SW. Small RNA-based antimicrobial immunity. Nat Rev Immunol. 2019;19(1):31–44.
15. Zhao JH, Guo HS. RNA silencing: from discovery and elucidation to application and perspectives. J Integr Plant Biol. 2022;64(2):476–98.
16. Borges F, Martienssen RA. The expanding world of small RNAs in plants. Nat Rev Mol Cell Biol. 2015;6(12):727–41.
17. Matzke MA, Mosher RA. RNA-directed DNA methylation: an epigenetic pathway of increasing complexity. Nat Rev Genet. 2014;15(6):394–408.
18. Creasey KM, Zhai J, Borges F, Van E, Regulski M, Meyers BC, Martienssen RA. miRNAs trigger widespread epigenetically activated siRNAs from transposons in Arabidopsis. Nature. 2014;508(7496):411–5.
19. Wu L, Zhou H, Zhang Q, Zhang J, Ni F, Liu C, Qi Y. DNA methylation mediated by a microRNA pathway. Mol Cell. 2010;38(3):465–75.
20. Ye R, Chen Z, Lian B, Rowley MJ, Xia N, Chai J, Li Y, He XJ, Wierzbicki AT, Qi Y. A Dicer-Independent Route for Biogenesis of siRNAs that Direct DNA Methylation in Arabidopsis. Mol Cell. 2016;61(2):222–35.
21. Fang X, Qi Y. RNAi in Plants: An Argonaute-Centered View. Plant Cell. 2016;28(2):272–85.
22. Vazquez F. Arabidopsis endogenous small RNAs: highways and byways. Trends Plant Sci. 2006;11(9):460–8.
23. Kapoor M, Arora R, Lama T, Nijhawan A, Khurana JP, Tyagi AK, Kapoor S. Genome-wide identification, organization and phylogenetic analysis of Dicer-like, Argonaute and RNA-dependent RNA Polymerase gene families and their expression analysis during reproductive development and stress in rice. BMC Genomics. 2008;9(1):1–17.
24. Qian Y, Cheng Y, Cheng X, Jiang H, Zhu S, Cheng B. Identification and characterization of Dicer-like, Argonaute and RNA-dependent RNA polymerase gene families in maize. Plant Cell Rep. 2011;30:1347–63.
25. Liu X, Lu T, Dou YC, Yu B, Zhang C. Identification of RNA silencing components in soybean and sorghum. BMC Bioinformatics. 2014;15(1):1–13.
26. Sabbione A, Daurelio L, Vegetti A, Talón M, Tadeo F, Dotto M. Genome-wide analysis of AGO, DCL and RDR gene families reveals RNA-directed DNA methylation is involved in fruit abscission in Citrus sinensis. BMC Plant Biol. 2019;19:1–13.

27. Wu J, Yang Z, Wang Y, Zheng L, Ye R, Ji Y, Zhao S, Ji S, Liu R, Xu L, Zheng H, Zhou Y, Zhang X, Cao X, Xie L, Wu Z, Qi Y, Li Y. Viral-inducible Argonaute18 confers broad-spectrum virus resistance in rice by sequestering a host microRNA. Elife. 2015;4.
28. Gan D, Zhan M, Yang F, Zhang Q, Hu K, Xu W, Lu Q, Zhang L, Liang D. Expression analysis of argonaute, Dicer-like, and RNA-dependent RNA polymerase genes in cucumber (Cucumis sativus L.) in response to abiotic stress. J Genet. 2017;96:235–49.
29. Zhai L, Teng F, Zheng K, Xiao J, Deng W, Sun W. Expression analysis of Argonaute genes in maize (Zea mays L.) in response to abiotic stress. Hereditas. 2019;156:1–10.
30. Cai XY, Fu JY, Li X, Peng L, Yang L, Liang Y, Jiang M, Ma J, Sun L, Guo B, Yu X. Low-molecular-weight organic acid-mediated tolerance and Pb accumulation in centipedegrass under Pb stress. Ecotoxicol Environ Saf. 2022;241:113755.
31. Hook JE, Hanna WW, Maw BW. Quality and growth response of centipedegrass to extended drought. Agron J. 1992;84(4):606–12.
32. Li J, Guo H, Zong J, Chen J, Li D, Liu J. Genetic diversity in centipedegrass [Eremochloa ophiuroides (Munro) Hack.]. Hortic Res. 2020;7:4.
33. Islam MA, Hirata M. Centipedegrass (Eremochloa ophiuroides (Munro) Hack.): growth behavior and multipurpose usages. Grassl Sci. 2005;1(3):183–90.
34. Johnson BJ, Carrow RN. Influence of soil pH and fertility programs on centipedegrass. Agron J. 1992;84(1):21–6.
35. Liu Y, Xiong Y, Zhao J, Bai S, Li D, Chen L, Feng J, Li Y, Ma X, Zhang J. Molecular Mechanism of Cold Tolerance of Centipedegrass Based on the Transcriptome. Int J Mol Sci. 2023;24(2):1265.
36. Katuwal KB, Xiao B, Jespersen D. Root physiological and biochemical responses of seashore paspalum and centipedegrass exposed to iso-osmotic salt and drought stresses. Crop Sci. 2020;60(2):1077–89.
37. Wang J, Zi H, Wang R, Liu J, Wang H, Chen R, Li L, Guo H, Chen J, Li J, Zong J. A high-quality chromosome-scale assembly of the centipedegrass [Eremochloa ophiuroides (Munro) Hack.] genome provides insights into chromosomal structural evolution and prostrate growth habit. Horticulture Research. 2021;8(2):201.
38. Gasteiger E, Hoogland C, Gattiker A, Duvaud SE, Wilkins MR, Appel RD, Bairoch A. Protein identification and analysis tools in the ExPASy server. Totowa, NJ. Humana Press. 2005:571–607.
39. Horton P, Park KJ, Obayashi T, Fujita N, Harada H, Adams-Collier CJ, Nakai K. WoLF PSORT: Protein Localization Predictor. Nucleic Acids Res. 2007;32(2):585–7.
40. Procter JB, Carstairs G, Soares B, Mourão K, Ofoegbu TC, Barton D, Lui L, Menard A, Sherstnev N, Roldan-Martinez D, Duce S, David M, Martin A, Barton GJ. Alignment of Biological Sequences with Jalview. US: Springer; 2021. p. 203–24.
41. Tamura K, Stecher G, Kumar S. MEGA11: molecular evolutionary genetics analysis version 11. Mol Biol Evol. 2021;38(7):3022–7.
42. Wang Y, Tang H, Debarry J, Tan X, Li J, Wang X, Lee T, Jin H, Marler B, Guo H, Kissinger JC, Paterson AH. MCScanX: a toolkit for detection and evolutionary analysis of gene synteny and collinearity. Nucleic Acids Res. 2012;40(7):49.
43. Holub EB. The arms race is ancient history in Arabidopsis, the wildflower. Nat Rev Genet. 2001;2(7):516.
44. Chen C, Wu Y, Xia R. A painless way to customize Circos plot: From data preparation to visualization using TBtools. Imeta. 2022;1(3).
45. Chen C, Wu Y, Li J, Wang X, Zeng Z, Xu J, Liu Y, Feng J, Chen H, He Y, Xia R. TBtools-II: A "One for All, All for One" Bioinformatics Platform for Biological Big-Data Mining. Mol Plant. 2023;16(11):1733–42.
46. Wang XY, Shu X, Su XL, Xiong YL, Xiong Y, Chen ML, Tong Q, Ma X, Zhang JB, Zhao JM. Selection of Suitable Reference Genes for RT-qPCR Gene Expression Analysis in Centipedegrass under Different Abiotic Stress. Genes. 2023;14(10):1874.
47. Schmittgen TD, Livak KJ. Analyzing real-time PCR data by the comparative CT method. Nat Protoc. 2008;3(6):1101–8.
48. Rivas FV, Tolia NH, Song JJ, Aragon JP, Liu J, Hannon GJ, Joshua-Tor L. Purified Argonaute2 and an siRNA form recombinant human RISC. Nat Struct Mol Biol. 2005;12(4):340–9.
49. Carbonell A, Fahlgren N, Garcia-Ruiz H, Gilbert KB, Montgomery TA, Nguyen T, Cuperus JT, Carrington JC. Functional analysis of three Arabidopsis ARGONAUTES using slicerdefective mutant. Plant Cell. 2012;24(9):3613–29.
50. Liu C, Axtell MJ, Fedoroff NV. The helicase and RNaseIIIa domains of Arabidopsis DICER-LIKE1 modulate catalytic parameters during microRNA biogenesis. Plant Physiol. 2012;159(2):748–58.
51. Hammond SM. Dicing and slicing: the core machinery of the RNA interference pathway. FEBS Lett. 2005;579(26):5822–9.
52. Zong J, Yao X, Yin J, Zhang D, Ma H. Evolution of the RNA-dependent RNA polymerase (RdRP) genes: duplications and possible losses before and after the divergence of major eukaryotic groups. Gene. 2009;447(1):29–39.
53. Cao JY, Xu YP, Li W, Li SS, Rahman H, Cai XZ. Genome-wide identification of DICER-LIKE, ARGONAUTE, and RNA-DEPENDENT RNA POLYMERASE gene families in Brassica species and functional analyses of their Arabidopsis homologs in resistance to Sclerotinia sclerotiorum. Front Plant Sci. 2016;7:1–17.
54. Waterhouse A, Bertoni M, Bienert S, Studer G, Tauriello G, Gumienny R, Heer FT, de Beer TAP, Rempfer C, Bordoli L. SWISS-MODEL: Homology Modelling of Protein Structures and Complexes. Nucleic Acids Res. 2018;46:296–303.
55. Bologna NG, Voinnet O. The diversity, biogenesis, and activities of endogenous silencing small RNAs in Arabidopsis. Annu Rev Plant Biol. 2015;65:473–503.
56. Singh RK, Gase K, Baldwin IT, Pandey SP. Molecular evolution and diversification of the Argonaute family of proteins in plants. BMC Plant Biol. 2015;15:1–16.
57. Zhang H, Xia R, Meyers BC, Walbot V. Evolution, functions, and mysteries of plant ARGONAUTE proteins. Curr Opin Plant Biol. 2015;27:84–90.
58. Rogers K, Chen X. Biogenesis, turnover, and mode of action of plant microRNAs. Plant Cell. 2013;25(7):2383–99.
59. Wu L, Zhang Q, Zhou H, Ni F, Wu X, Qi Y. Rice MicroRNA effect or complexes and targets. Plant Cell. 2009;21(11):3421–35.
60. Li Z, Li W, Guo M, Liu S, Liu L, Yu Y, Mo B, Chen X, Gao L. Origin, evolution and diversification of plant ARGONAUTE proteins. Plant J. 2022;109(5):1086–97.
61. Li Y, Huang Y, Pan L, Zhao Y, Huang W, Jin W. Male sterile 28 encodes an ARGONAUTE family protein essential for male fertility in maize. Chromosome Res. 2021;29:189–201.
62. Bélanger S, Zhan J, Meyers BC. Phylogenetic analyses of seven protein families refine the evolution of small RNA pathways in green plants. Plant Physiol. 2023;192(2):1183–203.
63. Havecker ER, Wallbridge LM, Hardcastle TJ, Bush MS, Kelly KA, Dunn RM, Schwach F, Doonan JH, Baulcombe DC. The Arabidopsis RNA-directed DNA methylation argonautes functionally diverge based on their expression and interaction with target loci. Plant Cell. 2010;22(2):321–34.
64. Zhou C, Han L, Fu C, Wen J, Cheng X, Nakashima J, Ma J, Tang Y, Tan Y, Tadege M, Mysore KS, Xia G, Wang ZY. The trans-acting short interfering RNA3 pathway and no apical meristem antagonistically regulate leaf margin development and lateral organ separation, as revealed by analysis of an argonaute7/lobed leaflet1 mutant in Medicago truncatula. Plant Cell. 2013;25(12):4845–62.
65. Margis R, Fusaro AF, Smith NA, Curtin SJ, Watson JM, Finnegan EJ, Waterhouse PM. The evolution and diversification of Dicers in plants. FEBS Letters. 2006;580(10):2442–50.
66. Henderson IR, Zhang X, Lu C, Johnson L, Meyers BC, Green PJ, Jacobsen SE. Dissecting Arabidopsis thaliana DICER function in small RNA processing, gene silencing and DNA methylation patterning. Nat Genet. 2006;38(6):721–5.
67. Voinnet O. Use, tolerance and avoidance of amplified RNA silencing by plants. Trends Plant Sci. 2008;13(7):317–28.
68. Nakazawa Y, Hiraguri A, Moriyama H, Fukuhara T. The dsRNA-binding protein DRB4 interacts with the Dicer-like protein DCL4 in vivo and functions in the trans-acting siRNA pathway. Plant Mol Biol. 2007;63(6):777–85.
69. Liu B, Li P, Li X, Liu C, Cao S, Chu C, Cao X. Loss of function of OsDCL1 affects microRNA accumulation and causes developmental defects in rice. Plant Physiol. 2005;139(1):296–305.
70. Xie Z, Johansen LK, Gustafson AM, Kasschau KD, Lellis AD, Zilberman D, Jacobsen SE, Carrington JC. Genetic and functional diversification of small RNA pathways in plants. PLoS Biol. 2004;2(5): e104.
71. Li J, Zhang BS, Wu HW, Liu CL, Guo HS, Zhao JH. The RNA-binding domain of DCL3 is required for long-distance RNAi signaling. aBIOTECH. 2023;5(1):114.

72. Brodersen P, Sakvarelidze-Achard L, Bruun-Rasmussen M, Dunoyer P, Yamamoto YY, Sieburth L, Voinnet O. Widespread translational inhibition by plant miRNAs and siRNAs. Science. 2008;320(5880):1185–90.
73. Patel P, Mathioni SM, Hammond R, Harkess AE, Kakrana A, Arikit S, Dusia A, Meyers BC. Reproductive phasiRNA loci and DICER-LIKE5, but not microRNA loci, diversified in monocotyledonous plants. Plant Physiol. 2021;185(4):1764–82.
74. Salse J, Bolot S, Throude M, Jouffe V, Piegu B, Quraishi UM, Calcagno T, Cooke R, Delseny M, Feuillet C. Identification and characterization of shared duplications between rice and wheat provide new insight into grass genome evolution. Plant Cell. 2008;20(1):11–24.
75. Murat F, Xu JH, Tannier E, Abrouk M, Guilhot N, Pont C, Messing J, Salse J. Ancestral grass karyotype reconstruction unravels new mechanisms of genome shuffling as a source of plant evolution. Genome Res. 2010;20(11):1545–57.
76. Chen S, Liu W, Naganuma M, Tomari Y, Iwakawa HO. Functional specialization of monocot DCL3 and DCL5 proteins through the evolution of the PAZ domain. Nucleic Acids Res. 2022;50(8):4669–84.
77. Song X, Li P, Zhai J, Zhou M, Ma L, Liu B, Jeong D, Nakano M, Cao S, Liu C. Roles of DCL4 and DCL3b in rice phased small RNA biogenesis. Plant J. 2012;69(3):462–74.
78. Teng C, Zhang H, Hammond R, Huang K, Meyers BC, Walbot V. Dicer-like 5 deficiency confers temperature-sensitive male sterility in maize. Nat Commun. 2020;11(1):2912.
79. Shoemaker RC, Polzin K, Labate J, Specht J, Brummer EC, Olson T, Young N, Concibido V, Wilcox J, Tamulonis JP, Kochert G, Boerma HR. Genome duplication in soybean (Glycine subgenus soja). Genetics. 1996;144(1):329–38.
80. Carmell MA, Xuan Z, Zhang MQ, Hannon GJ. The Argonaute family: tentacles that reach into RNAi, developmental control, stem cell maintenance, and tumorigenesis. Genes Dev. 2002;16(21):2733–42.
81. Schmitz RJ, Hong L, Fitzpatrick KE, Amasino RM. DICER-LIKE 1 and DICER-LIKE 3 redundantly act to promote flowering via repression of FLOWERING LOCUS C in Arabidopsis thaliana. Genetics. 2007;176(2):1359–62.
82. Qin L, Mo N, Zhang Y, Muhammad T, Zhao G, Zhang Y, Liang Y. CaRDR1, an RNA-dependent RNA polymerase plays a positive role in pepper resistance against TMV. Front Plant Sci. 2017;8:1063.
83. Law JA, Jacobsen SE. Establishing, maintaining and modifying DNA methylation patterns in plants and animals. Nat Rev Genet. 2010;11(3):204–20.
84. Hunter LJR, Brockington SF, Murphy AM, Pate AE, Gruden K, Macfarlane SA, Palukaitis P, Carr JP. RNA-dependent RNA polymerase 1 in potato (Solanum tuberosum) and its relationship to other plant RNA-dependent RNA polymerases. Sci Rep. 2016;6(1):23082.
85. Xia R, Xu J, Meyers BC. The Emergence, Evolution, and Diversification of the miR390-TAS3-ARF Pathway in Land Plants. Plant Cell. 2017;29(6):1232–47.

Publisher's Note